Detection of bifurcations in noisy coupled systems from multiple time series

Mark S. Williamson and Timothy M. Lenton

Citation: Chaos: An Interdisciplinary Journal of Nonlinear Science **25**, 036407 (2015); doi: 10.1063/1.4908603
View online: http://dx.doi.org/10.1063/1.4908603
View Table of Contents: http://scitation.aip.org/content/aip/journal/chaos/25/3?ver=pdfcov
Published by the AIP Publishing

Detection of bifurcations in noisy coupled systems from multiple time series

Mark S. Williamson[a] and Timothy M. Lenton
Earth System Science Group, College of Life and Environmental Sciences, University of Exeter, Laver Building, North Park Road, Exeter EX4 4QE, United Kingdom

(Received 8 September 2014; accepted 2 February 2015; published online 18 February 2015)

We generalize a method of detecting an approaching bifurcation in a time series of a noisy system from the special case of one dynamical variable to multiple dynamical variables. For a system described by a stochastic differential equation consisting of an autonomous deterministic part with one dynamical variable and an additive white noise term, small perturbations away from the system's fixed point will decay slower the closer the system is to a bifurcation. This phenomenon is known as critical slowing down and all such systems exhibit this decay-type behaviour. However, when the deterministic part has multiple coupled dynamical variables, the possible dynamics can be much richer, exhibiting oscillatory and chaotic behaviour. In our generalization to the multi-variable case, we find additional indicators to decay rate, such as frequency of oscillation. In the case of approaching a homoclinic bifurcation, there is no change in decay rate but there is a decrease in frequency of oscillations. The expanded method therefore adds extra tools to help detect and classify approaching bifurcations given multiple time series, where the underlying dynamics are not fully known. Our generalisation also allows bifurcation detection to be applied spatially if one treats each spatial location as a new dynamical variable. One may then determine the unstable spatial mode(s). This is also something that has not been possible with the single variable method. The method is applicable to any set of time series regardless of its origin, but may be particularly useful when anticipating abrupt changes in the multi-dimensional climate system. © *2015 AIP Publishing LLC*.
[http://dx.doi.org/10.1063/1.4908603]

Abrupt changes in complex systems such as the human body, ecosystems, or the climate system can have unwelcome and expensive consequences. Ideally, given one or more time series of some measurable variables, one would like an early warning method to indicate whether an abrupt change is imminent. Abrupt changes can result from crossing a bifurcation in the underlying dynamical system. Recently, there has been a burgeoning body of work on the detection of approaching bifurcation in noisy systems whose deterministic dynamics are assumed to be approximated by a first order ordinary differential equation (ODE) of one dynamical variable. These methods work by looking for the system's recovery from noisy perturbations becoming more sluggish, a phenomenon known as critical slowing down. This is a generic feature of approaching bifurcations in systems modelled by autonomous first order differential equations of one dynamical variable with additive white noise, where the behaviour is decay toward a fixed point. However, it is not always possible to approximate parts of a complex system in such reduced manner. For example, the climate system can display coupled, oscillatory, or chaotic behaviour. Here, we make a direct generalization of the one dynamical variable model to many dynamical variables. We find in addition to an indicator related to the critical slowing down, we get an indicator related to the system's oscillation frequency. These techniques may allow one not only to detect the approach of a wider range of bifurcations but also the type of bifurcation being approached, and therefore an indication of what the system may do in the future. The generalization also allows bifurcation detection to be applied spatially if one treats each spatial location as a new dynamical variable (each spatial location generates its own time series) and identification of the dominant spatial unstable modes of the system.

I. INTRODUCTION

The potential for early warning of an approaching abrupt change, or "tipping point," in a complex, dynamical system has been the focus of much recent research, reviewed elsewhere.[1–3] Abrupt change in a dynamical system can occur due to a bifurcation. That is, a small smooth change made in parameter values can result in a sudden or topological change in the space of steady state solutions. One method of detecting an approaching bifurcation is to perform repeatable experiments on the system itself and study its responses.[4–6] This is very hard or impossible to do with large, complex systems, such as the climate, so one may instead build models of varying complexity and perform experiments on these models instead.[7,8] A third approach is to look at the statistics of some measurable variable of the system, usually a time series of this variable, as these may reveal something about the future behaviour without the need for a detailed model of the system.[1–3] All three approaches are potentially useful

[a]Electronic mail: m.s.williamson@exeter.ac.uk

sources of information, particularly when taken together. It is the third approach, we develop in this paper.

Much work on the anticipation of bifurcations from a time series, e.g., in ecosystems[1] or the climate system,[2,9] has been based on the following assumptions: (i) the system being studied is approximately in a steady state (or equilibrium). (ii) Changes in the equilibrium state structure are due to some slowly varying control parameter, α, that can be treated as a constant compared to the timescale of the system's dynamics, formally $\tau \gg \dot{\alpha}$, where τ is the e-folding time of the system (to be defined later in the paper) and over-dots denote differentiation with respect to time. This effectively means that the system stays in a steady state as the underlying steady state structure slowly changes. (iii) The system's deterministic dynamics can be described by an autonomous first order ODE with one dynamical variable to a good approximation. Other variables can be modelled as uncorrelated noise with zero mean drawn from a Gaussian distribution. (iv) The amplitude of this noise is small compared to the separation between steady states such that the dynamics is described by the evolution of the steady state manifold rather than noise induced transitions between steady states. It is also small enough that the dynamics caused by noisy perturbations away from steady state are well approximated by the linearized dynamics. (v) The abrupt change in the system is due to a bifurcation.

Under these assumptions, critical slowing down is expected prior to a bifurcation. This can be visualised by thinking of the state of the system as a point on a slowly varying potential. An example of a possible potential is shown in Figure 1. Provided the system has a stable fixed point, one can imagine this potential having a well, with the stable fixed point located at the lowest point of the well. If the system is initially located at some point on the slopes of this well it will try to minimize the value of its potential, moving from the large values on the slopes to smaller values closer to the bottom. As the potential is slowly changed by varying some control parameter α, the location of the fixed point will slowly change too and provided the system responds faster than α is varied, it will remain sitting very close to the changing fixed point. As α is slowly changed towards a bifurcation the sides of the well get shallower around the neighborhood of the fixed point and the restoring force to any perturbation of the system, proportional to the gradient, will get weaker. The perturbation will not decay toward the fixed point as quickly, until at the point of bifurcation, the potential becomes flat and the fixed point is on the edge of going from stable to unstable. The approach of the bifurcation will therefore show up as weakening of the decay rate until it goes to zero at the bifurcation. It is this generic feature of a gradient system—noting that all autonomous first order ODEs of one variable are such systems—that one tries to detect as an early warning.

Using this framework, Held and Kleinen[10] showed that simulated abrupt changes in the ocean's thermohaline circulation can be anticipated. The model fitted to the time series was an iterative map with a white noise term equivalent to a first order ODE with an added white noise term known as an autoregressive model of order 1 (often written AR(1) as shorthand). This approach[10] has provided the foundation for much subsequent work. For example, in the climate field, early warnings have been found in more complex numerical models approaching a collapse of the thermohaline circulation.[11–13] Applications to paleo-climate data have shown early warning signals prior to at least some abrupt climate changes in Earth's history.[9,11,14] An ongoing debate surrounds whether abrupt climate changes during the last ice age, known as Daansgard Oeschger events, showed bifurcation-type early warning signals.[15,16] There are also examples of the method failing, for example, in the case of simulated Amazon dieback,[17] where assumption (ii) is violated.

In this paper, we relax assumption (iii), that is, we look at systems whose deterministic behaviour cannot be

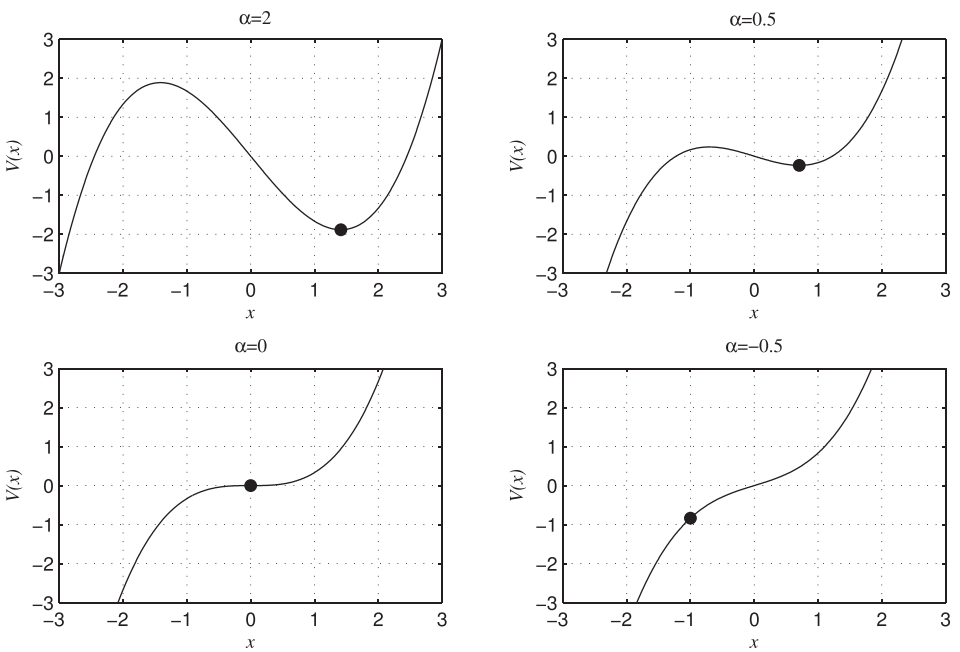

FIG. 1. Changing potential caused by varying α slowly for the system $\dot{x} = \alpha - x^2$. The potential is given by $V(x) = -\frac{d\dot{x}}{dx}$ and fixed points are $x^* = \pm\sqrt{\alpha}$ for $\alpha > 0$. The current state of the system is given by the black dot. In the upper left hand panel, there is a stable fixed point (at $x^* = \sqrt{2}$) located at the bottom of the potential well and the system is sitting close to it. In the upper right hand panel, as α is slowly varied, the well gets shallower and the walls less steep causing small perturbations away from the stable fixed point (at $x^* = \sqrt{1/2}$) to decay more slowly. In the lower left hand panel, there is a saddle-node bifurcation where the fixed point is on the cusp of being unstable. Even the smallest perturbation away from the fixed point will not decay. In the lower right hand panel, α is changed so there are no longer any fixed points and the system runs off to infinity.

described by autonomous first order ODEs of one dynamical variable effectively. These are systems that can display much richer dynamics such as oscillatory or chaotic behaviour, dynamics that cannot occur in autonomous first order ODEs of one dynamical variable. We do this by simply extending the method based in all the previous works mentioned to first order ODEs of multiple dynamical variables with additive white noise. This method is also sufficiently general to describe the dynamics of second and higher order ODEs of one dynamical variable, and nonautonomous systems, by making a simple change of variables.

These techniques are all based on fitting noisy linear models to a time series so essentially one is reconstructing the system's Jacobian (a matrix of linearization constants) around a point in its phase space. Studying a system's Jacobian is the main tool for analysis of the stability of steady solutions. For systems modelled by one deterministic dynamical variable, the eigenvalue of the Jacobian goes from negative real values through zero at the bifurcation as the system's fixed point loses stability resulting in the critical slowing down. When a system consists of two or more dynamical variables, the Jacobian now has multiple eigenvalues which can be complex, resulting in many more possible behaviours. The real part of one or more of these eigenvalues can pass from negative values through zero at a bifurcation destabilising the fixed point analogously to the one variable case showing up as critical slowing down. Bifurcations that feature this critical slow down are classed as local bifurcations. However, another possibility is that the real parts of the Jacobian's eigenvalues remain invariant as it passes through a bifurcation so that no critical slowing down is observed. These are classed as global bifurcations. The imaginary parts of the eigenvalues may however be changing and this can be used as an additional indicator. We give an example of such a global bifurcation, the homoclinic bifurcation, in Sec. IV. A lot is known about the behaviour of the eigenvalues of the Jacobian for many classes of dynamical systems and bifurcations, and there are many good texts such as Strogatz[18] and Kuznetsov[19] one may consult for more details.

In the real world, there are typically a very large number of, or infinitely many, coupled dynamical variables influencing the variable one is interested in (we refer to the dynamical variable of interest as "the system"). But when using these statistical techniques, one generally wants to fit a minimal model, simplicity being a key factor in the appeal of these methods. In light of this, ideally one would want to use a model based on a first order ODE of one dynamical variable to fit to one's time series and approximate all the other dynamical variables affecting the system as an additive white noise term (if the variables are fast relative to the system) or as a control parameter (if the variables are slow). This is generally not possible when the dynamics is dominated by coupled behaviour over the timescale of interest. Technically, this happens when the dominant eigenmodes of the linearized system have associated eigenvalues with imaginary parts that are of similar size or larger than their real parts. One would then have to "enlarge" the system to more than one dynamical variable for the model to reproduce this coupled behaviour. We will provide examples of such systems in Sec. IV.

To illustrate this timescale dependence, even though a system may show oscillatory behaviour, one may still be able to describe the deterministic part as a first order ODE in one dynamical variable if the oscillation frequency is small compared to the decay timescale. An example are the relaxation oscillations (an oscillatory cycle described by a slow build up and a fast discharge) often used to model past climate dynamics.[20,21] Rather than being treated as a coupled, oscillatory phenomena, the slow build up in the relaxation oscillation is treated as a slowly varying parameter and the rapid discharge as a bifurcation on this slow manifold.

One should also note that abrupt changes are not always due to bifurcations. For example, transitions between multiple steady states may be induced by "large" amplitude noise, large here meaning that the probability of a perturbation large enough to push the system into a different state over the timescale of interest is non-negligible. These noisy transitions have been studied in the context of Dansgaard Oeschger events.[15]

The paper is organised as follows: In Sec. II, we review the method used to detect bifurcations applicable to systems whose deterministic dynamics is effectively modelled by autonomous first order ODEs of one dynamical variable. In Sec. III, we directly generalize this method to systems described by multiple first order ODEs. We illustrate the general method in Sec. IV with examples of two particular bifurcations, before concluding in Sec. V.

II. BIFURCATION DETECTION IN NOISY GRADIENT SYSTEMS

For a system modelled by

$$\dot{x} = f(x), \tag{1}$$

where $\dot{x} \equiv \frac{dx}{dt}$ and $f(x)$ is some, in general, nonlinear function of x one can always write down the potential function, $V(x)$, by directly integrating $f(x) = -\frac{\partial V}{\partial x}$, i.e., the dynamics is given by the gradient of some function V. These are known as gradient systems. However, for multivariable dynamics, one may not always be able to write the dynamical variables x_i as the gradient of V, $\frac{dx_i}{dt} = -\frac{\partial V}{\partial x_i}$. A consequence of being able to write the dynamics in terms of V is that the Jacobian is real and symmetric and therefore constrained to have real eigenvalues. This restricts the dynamics, making oscillating solutions impossible in such a system. At present, we restrict to one dynamical variable and therefore can find V.

A. Exponential decay constant as a fitted parameter of an autoregressive (AR) model

In previous work, it is assumed that the system of interest has one dynamical variable described by a stochastic differential equation consisting of an autonomous first order differential equation plus some Gaussian white noise, i.e.,

$$\dot{x} = f(x) + \xi(t), \tag{2}$$

where $\xi(t)$ is a continuous Gaussian white noise process (an independent random variable drawn from a normal distribution with zero mean and variance σ^2 independent of time, see Refs. 22 and 23 for formal definitions). It is uncorrelated with itself at differing times. One also assumes the system is in or close to a fixed point and the noise amplitude is small so that a Taylor expansion of $f(x)$ to first order is a good approximation around the fixed point x^* $(f(x^*) = 0)$

$$\dot{x} \approx \left.\frac{\partial f}{\partial x}\right|_{x=x^*} (x - x^*) + \xi(t). \tag{3}$$

Terms of the order $(x - x^*)^2$ and greater are neglected, since they are assumed to be small relative to the first order term in the expansion. One then discretizes the time to a step of length Δt, using the Euler-Maruyama method[24] and rearranges the equation so that

$$x_{m+1} = ax_m + c + \varepsilon_{m+1}, \tag{4}$$

where $x_m = x(t_m)$, $\varepsilon_m = \sqrt{\Delta t}\xi(t_m)$, and $t_m = t_0 + m\Delta t$. c and a are constants and can be identified as

$$a = 1 + J(x^*)\Delta t \sim \exp[J(x^*)\Delta t], \tag{5}$$

$$c = -x^* J(x^*)\Delta t. \tag{6}$$

$J(x^*) \equiv \frac{\partial f}{\partial x}|_{x=x^*}$ is the Jacobian evaluated at x^*. The expectation value of the Gaussian white noise satisfies $E(\varepsilon_m \varepsilon_n) = \delta_{mn}\sigma^2 \Delta t$. Equation (4) is known as an autoregressive model of order 1 usually written as AR(1) (see for example, Ref. 25). We wish to fit this model to a time series of some variable $(x_1, x_2, ..., x_{M-1}, x_M)$. We are particularly interested in determining the value of a, since it is proportional to the exponential decay constant $a \sim \exp(\lambda \Delta t)$, $\lambda \sim J(x^*) = -\frac{\partial^2 V}{\partial x^2}$ is the exponential decay constant (sometimes referred to as decay rate for brevity) and is the negative inverse of the system's e-folding time $\tau = -\frac{1}{\lambda}$, the timescale of the system. One can find a by multiplying both sides of Eq. (4) by x_m and taking expectation values so that

$$a = \frac{E(x_{m+1}x_m) - \mu^2}{E(x_m^2) - \mu^2}, \tag{7}$$

which can be recognised as the lag 1 autocorrelation of the time series. $\mu = E(x_m)$ is the mean of the time series. In deriving this result, we have assumed the mean is independent of time, $E(x_m) = E(x_{m+1})$, i.e., it is a stationary process.

It is worth looking at the solution of Eq. (4) to gain some intuition for its behaviour. Writing out the solutions for each time step explicitly, one finds that

$$x_m = a^m x_0 + \sum_{i=1}^{m-1} a^i \varepsilon_{m-i}, \tag{8}$$

if one assumes $\mu = 0$ implying $c = 0$ and $x^* = 0$. The solution has two parts, one deterministic depending on the initial condition, x_0 and one stochastic, the sum of the random noise terms. The constant a, provided it is less than 1, acts to decay the system from its initial point to zero in the deterministic part and also acts to decay the noise terms; the farther back in time they are, the more they are decayed. As $a \to 1$ $(\lambda \to 0)$ and we approach a bifurcation, decay is reduced until at $a = 1$, we have a pure random walk.

To check whether the decay rate in a given a time series of M points is decreasing, one starts by choosing a window of m consecutive points $x_1, x_2, ..., x_m$, where $m < M$ and estimates a for this window which we label a_1. One usually uses a sliding window and calculates a for the set of m points $x_2, x_3, ...x_n, x_{m+1}$ giving a_2. This procedure is iterated until we have the set $a_1, a_2, ..., a_{M-m}$ from which one can determine whether the series of estimated $\{a_i\}$ is increasing (equivalent to decay rate decreasing) indicating the approach of a bifurcation.

B. Applying the method in practice

How one chooses the window parameters depends on timescales, uncertainty and from a more practical perspective, availability and resolution of data. Ideally one would choose $T_{window} \gg \tau \gg \Delta t$, where $T_{window} = m\Delta t$. Uncertainty via the standard error in the estimated parameters scales approximately as $1/\sqrt{m}$ making it desirable to take larger values of m to give more confidence in the estimation (the standard error can be calculated using Eq. (23)). However, if m is too large one may bias the estimated parameters as the change in the control parameter α over the time window may be large. Theoretically then higher temporal resolution and larger numbers of data are desirable. In practice, when analysing something like a historical climate data record Δt and m are fixed.

Note that Eq. (7) only applies to time series that are stationary. That is, the estimated mean should be independent of which part of the window it is calculated for. This may require removal of any trend within each window to give an approximately stationary series well modelled by an AR(1) process.

One may also estimate a using other fitting methods such as least squares or maximal likelihood estimation. One can show these two methods are equivalent to Eq. (7) in this case.[26]

III. GENERALIZATION TO MULTIPLE VARIABLES

In this section, we generalize the method in Sec. II to the multivariable case. The method is to reduce a set of N coupled, nonlinear stochastic equations to a set of N uncoupled (independent) AR(1) processes each of which can be treated the same as the single variable case outlined in Sec. II. The only difference is that the AR(1) model variables and parameters may be complex rather than purely real. We will also be more interested in the eigenvalues, λ_i, of the Jacobian matrix for the multivariable case as their behaviour has been well studied in nonlinear dynamics.[18,27] These are related to the eigenvalues of the AR(1) matrix A, $\{\tilde{a}_1, \tilde{a}_2, .., \tilde{a}_N\}$ as $\tilde{a}_i \sim \exp(\lambda_i \Delta t)$.

We consider a set of N (generally) coupled stochastic equations of N dynamical variables each labelled by $x^{(i)}$, $i = 1, 2, ..., N-1, N$

$$\dot{x}^{(i)} = f^{(i)}(x^{(1)}, x^{(2)}, ..., x^{(N-1)}, x^{(N)}) + \xi^{(i)}(t), \tag{9}$$

where the $f^{(i)}$ are in general complicated nonlinear functions of all the dynamical variables and $\xi^{(i)}(t)$ is a Gaussian white noise process continuous in time (a random variable drawn from a Gaussian distribution with standard deviation $\sigma^{(i)}$ and zero mean). The superscript (i) in parentheses indicates a label and not a power. The white noise terms are independent of each other and at different times. We note that this set of equations is sufficiently general to include nonlinear differential equations of order N by identifying time derivatives as new variables. For example, the third order differential equation in time with variable x, $\dddot{x} + \ddot{x} + \dot{x} + x = 0$, can be written as the set of three first order differential equations $\dot{x} = y$, $\dot{y} = z$, $\dot{z} = -(x + y + z)$. One may also handle non-autonomous systems, systems where $f^{(i)}$ depends explicitly on t, by also adding t as a new dynamical variable and an extra dynamical equation.

Analogously to the single variable case, we perform a Taylor expansion to first order around the point $\mathbf{x}_* = (x_*^{(1)}, x_*^{(2)}, ..., x_*^{(N)})$ on all N equations

$$\dot{x}^{(i)} \approx f^{(i)}(\mathbf{x}_*) + \sum_{j=1}^{N} \frac{\partial f^{(i)}}{\partial x^{(j)}}\bigg|_{\mathbf{x}=\mathbf{x}_*} \left(x^{(j)} - x_*^{(j)}\right) + \xi^{(i)}(t), \tag{10}$$

assuming that the noise amplitude and the first order terms approximate $f^{(i)}$ well. We define the vector $\mathbf{x} = (x^{(1)}, x^{(2)}, ..., x^{(N)})$. We then once again discretize the time step and rearrange to get a set of linear, coupled equations with added white noise (satisfying $E(\varepsilon_m^{(i)}\varepsilon_n^{(j)}) = \delta_{ij}\delta_{mn}(\sigma^{(i)})^2\Delta t$, where $\varepsilon_m^{(i)} = \sqrt{\Delta t}\xi^{(i)}(t_m)$)

$$\begin{aligned}
x_{m+1}^{(1)} &= a_{11}x_m^{(1)} + a_{12}x_m^{(2)} + ...a_{1N}x_m^{(N)} + c^{(1)} + \varepsilon_{m+1}^{(1)} \\
x_{m+1}^{(2)} &= a_{21}x_m^{(1)} + a_{22}x_m^{(2)} + ...a_{2N}x_m^{(N)} + c^{(2)} + \varepsilon_{m+1}^{(2)} \\
&\vdots \\
x_{m+1}^{(N)} &= a_{N1}x_m^{(1)} + a_{N2}x_m^{(2)} + ...a_{NN}x_m^{(N)} + c^{(N)} + \varepsilon_{m+1}^{(N)},
\end{aligned}$$

which can be written more succinctly as

$$\mathbf{x}_{m+1} = A\mathbf{x}_m + \mathbf{c} + \varepsilon_{\mathbf{m}+1}, \tag{11}$$

where A is a matrix of coupling constants, $\mathbf{c}$ is a vector of constants, and $\varepsilon_{\mathbf{m}}$ is a vector of independent white noise terms. Written in terms of the Jacobian, $J_{ij}(\mathbf{x}) = \frac{\partial f^{(i)}}{\partial x^{(j)}}|_{\mathbf{x}}$, A and $\mathbf{c}$ are

$$A = \mathbf{I} + J(\mathbf{x}_*)\Delta t \sim \exp[J(\mathbf{x}_*)\Delta t], \tag{12}$$

$$\mathbf{c} = [\mathbf{f}(\mathbf{x}_*) - J(\mathbf{x}_*)\mathbf{x}_*]\Delta t, \tag{13}$$

where $\mathbf{I}_{ij} = \delta_{ij}$ is the identity matrix and $\mathbf{f}(\mathbf{x})$ is a vector with ith component $f^{(i)}(\mathbf{x})$. Equation (11) is the multivariable AR(1) generalization of Eq. (4), and we wish to fit this model to the time series of N different variables each with M points. To find an estimator of A from the N different time series, we multiply both sides of Eq. (11) on the right by $\mathbf{x}_m^\dagger$ and take expectation values. The superscript † denotes the operation transposition. A can be found as

$$A = B\Sigma^{-1}, \tag{14}$$

where B is analogous to the the lag 1 covariance and Σ is the covariance matrix. The superscript -1 denotes matrix inversion. Both matrices are given explicitly by

$$\begin{aligned}
B &= E(\mathbf{x}_{m+1}\mathbf{x}_m^\dagger) - \mu\mu^\dagger, \\
\Sigma &= E(\mathbf{x}_m\mathbf{x}_m^\dagger) - \mu\mu^\dagger, \\
\mu &= E(\mathbf{x}_m).
\end{aligned} \tag{15}$$

Again, in deriving this result, we have assumed the mean is independent of time.

In the one variable case, A was a single number proportional to the exponential decay constant whereas in the multivariable case we have a coupling matrix. We want to find something analogous to the decay constant in the multivariable case. One can do this by making a change to some new basis of dynamical variables $\mathbf{x} \to \tilde{\mathbf{x}}$ such that expressed in this new basis $A \to \tilde{A}$ is diagonal, and therefore the N dynamical equations labelled by i are uncoupled (tildes denote variables in the uncoupled basis), i.e.,

$$\tilde{x}_{m+1}^{(i)} = \tilde{a}_i\tilde{x}_m^{(i)} + \tilde{c}^{(i)} + \tilde{\varepsilon}_{m+1}^{(i)}. \tag{16}$$

Each equation can then be treated exactly as in Sec. II, since each equation consists of just one dynamical variable and $\tilde{a}_i$ is just a number. To determine this change of basis simply amounts to finding the eigenvalues $(\tilde{a}_i)$ and eigenvectors of A. In other words, we look to decompose A as

$$A = U^{-1}\tilde{A}U, \tag{17}$$

where the rows of U are the eigenvectors of A, and $\tilde{A}$ is a diagonal matrix whose entries on the diagonal are the eigenvalues of A. One can always make this decomposition provided the determinant of A is non zero and all eigenvalues are different. If the determinant is zero, one may still be able to make this decomposition over the range of A indicating the system can be described by rank $(A) < N$ dynamical variables. If two or more eigenvalues are the same one may or may not be able to decompose A in this way. In the generic case, however, this decomposition does exist. The new variables $\tilde{x}^{(i)}$ in terms of the old variables are therefore given by

$$\tilde{\mathbf{x}} = U\mathbf{x}, \tag{18}$$

and there are analogous transformations to find $\tilde{c}$ and $\tilde{\varepsilon}$.

We are more interested in the eigenvalues of A. A is a matrix of real numbers however its eigenvalues and eigenvectors may be complex when A is not symmetric. When all eigenvalues are real (and therefore so are the eigenvectors meaning the new dynamical variables are also real), we have exactly the same situation as in Sec. II but rather than one, there are N independent, uncoupled AR(1) processes, each with it's own decay constant proportional to $\tilde{a}_i$ and one can look for increasing $\tilde{a}_i$ using a sliding window. In this case,

the system can only have decay type behaviour since it is analogous to N independent first order ODEs of one dynamical variable.

When there are complex eigenvalues (and corresponding complex eigenvectors), we again have N independent AR(1) processes except that each independent AR(1) process is a function of the real and imaginary parts of the new variables, i.e., it is essentially two dimensional, moving in the complex plane, rather than the real line and this gives rise to oscillations on the real and imaginary lines. Physically, complex eigenvalues are expressing the fact that the system is coupled. One can make a polar decomposition of each eigenvalue, $\tilde{a}_j$, as

$$\tilde{a}_j = |a_j| e^{i\phi_j}, \tag{19}$$

the product of the magnitude of the eigenvalue $|a_j|$ (a real number, analogous to a in Sec. II) and a phase factor $e^{i\phi_j}$ (here $i = \sqrt{-1}$ is the imaginary unit). The phase term, ϕ_j, is the new indicator and proportional to oscillation frequency of this coupled part of the system. This becomes clearer when one writes out each term explicitly for each time step as we did in Eq. (8). Dropping the label for each of the N equations and looking at just one with a corresponding complex eigenvalue and eigenvector, we have

$$\begin{aligned} \tilde{x}_1 &= |a| e^{i\phi} \tilde{x}_0 \\ \tilde{x}_2 &= |a|^2 e^{2i\phi} \tilde{x}_0 \\ \tilde{x}_3 &= |a|^3 e^{3i\phi} \tilde{x}_0 \\ &\vdots \\ \tilde{x}_m &= |a|^t e^{i\phi m} \tilde{x}_0. \end{aligned} \tag{20}$$

This sequence is plotted in Figure 2 for particular values. We have also neglected noise as being small $\tilde{\varepsilon} \sim 0$ in this example to show the deterministic behaviour of the model and also set $\tilde{c} = 0$. Adding noise will distort the spiral around the origin of the complex plane. Note that damped oscillations correspond to $|a| < 1$ and as $|a| \to 1$ we have free undamped oscillations. If $|a| > 1$, the oscillations grow in amplitude. ϕ is proportional to the oscillation frequency, rotating each successive point by ϕ radians on each time step. The larger ϕ is, the higher the oscillation frequency. Plotting the real and imaginary parts of this sequence (i.e., projecting the orbits in the complex plane on to the real and imaginary axes), we see damped, sinusoidal oscillations in Figure 3.

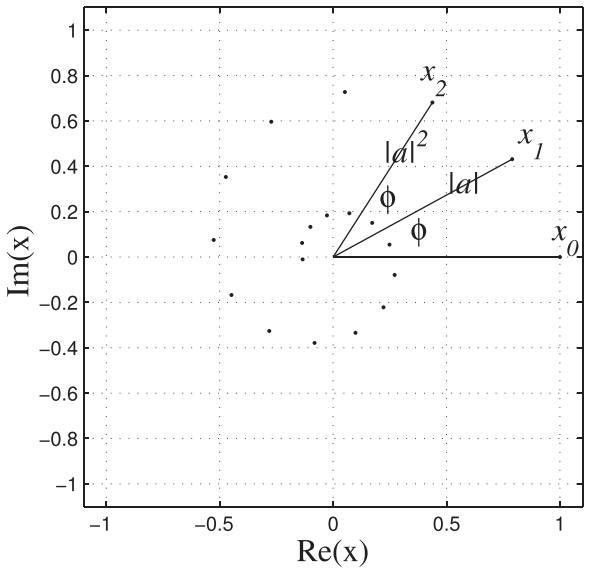

FIG. 2. The sequence of Eq. (20) plotted on the complex plane with $|a| = 0.9$, $\phi = 0.5$, $m = 19$, and $x_0 = 1$. This corresponds to a damped oscillation with decay rate $\log 0.9 \approx -0.11$ and frequency $\phi = 0.5$. This is visible when this spiral is plotted onto the real and imaginary axes in Figure 3.

A more familiar picture in which to classify bifurcations is using the motion of the eigenvalues of the Jacobian on the complex plane. The Jacobian's eigenvalues, λ_j, are related to the eigenvalues of A simply by $\tilde{a}_j = \exp(\lambda_j \Delta t)$; therefore the real part of λ_j is

$$\mathbb{R}(\lambda_j) = \frac{1}{\Delta t} \log |a_j|, \tag{21}$$

which is equivalent to the exponential decay constant while the imaginary part

$$\mathbb{I}(\lambda_j) = \frac{\phi_j}{\Delta t}, \tag{22}$$

is the frequency of oscillation. One can now reconstruct the system's Jacobian and look for changes that might suggest the approach of a bifurcation. We illustrate this method with examples in Sec. IV.

A. Calculation of standard errors in the entries of *A* and the eigenvalues of *A*

One can calculate the standard errors in each of the fitted parameters from a time series window of m points. Here, we give the explicit form for the standard errors, $\hat{\sigma}_{A_{ij}}$, in the estimation of the elements of the matrix A without derivation

$$\hat{\sigma}_{A_{ij}} = \sqrt{\frac{1}{m}\left[(\Sigma^{-1})_{ii}\Omega_{jj}\right]}, \tag{23}$$

where Σ is the covariance matrix defined in (15) and $\Omega = E(\varepsilon_{\mathbf{m}} \varepsilon_{\mathbf{m}}{}^{\dagger})$ is the covariance matrix of the white noise given explicitly as

$$\Omega = \Sigma - B\Sigma^{-1}B^{\dagger}. \tag{24}$$

A derivation of this result can be found in a more general setting in Lütkepohl.[26] One can then propagate the errors through to the calculation of the eigenvalues. In the general case of $N \leq 3$, there are known algebraic forms for calculation of the eigenvalues from the elements of A and the propagation of the errors can be done exactly. For $N > 3$, these general forms do not exist and usually the best one can do is provide a worst case bound on the error of the eigenvalues. More details can be found on these bounds in Wilkinson.[28]

B. Applying the method in practice

Everything mentioned in Sec. II B also applies for the multivariable case. We just add one more remark about choosing sliding window sizes based on timescales:

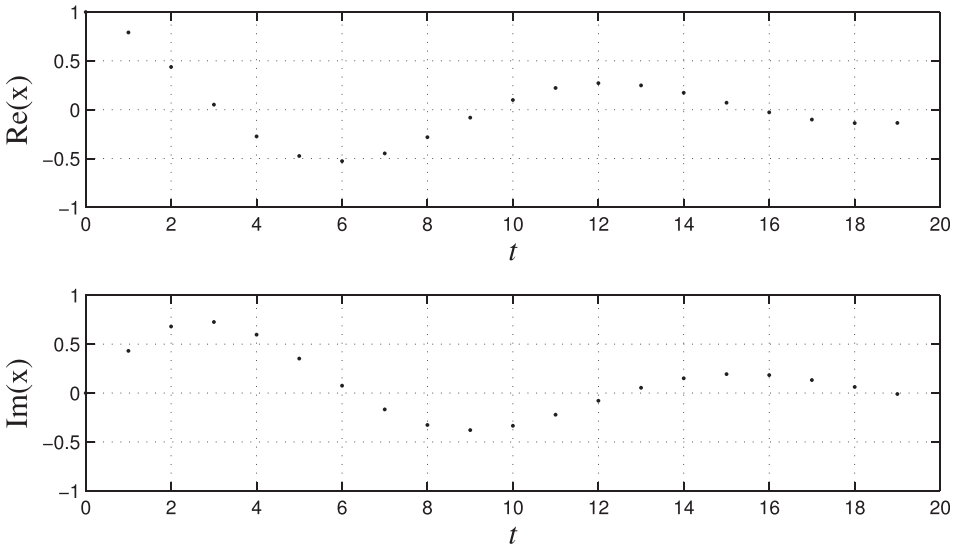

FIG. 3. Damped oscillations on the complex plane from Figure 2 projected onto the real and imaginary axes.

Assuming one has a coupled, oscillating system implies that the size of the oscillation term, $O(|\phi_j|)$, is comparable to or larger than the decay/growth term $O\left(\frac{1}{\Delta t}\log|a_j|\right)$. If the real part of the Jacobian's eigenvalue was much greater in magnitude, it would swamp the signal from the oscillatory part and the system would be well approximated by uncoupled AR(1) processes. One would therefore like to choose $T_{window} \gg \frac{\Delta t}{\phi} \gg \Delta t$. Note that there could be oscillations of many different frequencies in an N equation system from each of the N eigenmodes which may have an impact on choice, but in practice one would probably perform a separate analysis for each timescale assuming the slow variables are slowly varying constants for the fast timescale analysis, and the fast variables are noise for the slow variable analysis providing one can make such a separation.

As N grows, so the number of parameters to fit also grows. There are N^2 matrix elements in A and N numbers in each of $\mathbf{c}$ and $\sigma^{(i)}$ giving a total of $N(N+2)$ parameters to estimate. If there are m points in each time series window for each of the N dynamic variables, one may think there may only be $m/(N+2)$ points to estimate each parameter and this may limit the size of N or m. It is the scaling of number of parameters in A that is the problem. However, not all of these N^2 parameters are independent, it is only the N eigenvalues that are independent. These may be complex meaning two parameters describe each eigenvalue giving $4N$ free parameters in total, but complex eigenvalues always occur in conjugate pairs taking the number of parameters back to $3N$ and therefore giving $m/3$ points per parameter which is independent of N.

IV. EXAMPLES

In this section, we illustrate the methods described above by taking two examples of a specific set of dynamical equations exhibiting a particular type of bifurcation. We first describe the behaviour of those equations and following this pretend we do not know the form of these equations, we only have access to a set of time series, and apply our method in an attempt to reconstruct the Jacobian of the system. Our examples are both $N=2$ but the method is applicable to any N.

Explicitly, in the following examples we (i) numerically integrate Eqs. (26) and (29) with respect to time and added white noise term, i.e., for Eq. (26), $\dot{x} = y \to y + \xi^{(x)}$, $\dot{y} = \alpha - x^2 \to \alpha - x^2 + \xi^{(y)}$, where the standard deviation of the noise terms is equal and given by σ with slowly varying control parameter α. (ii) Record $x(t)$ and $y(t)$ at time interval between values of t, Δt to create the time series plotted in Figures 6 and 8. (iii) Apply Eqs. (14) and (15) to the m consecutive data points starting at x_i and y_i in a window of length $T_{window} = m\Delta t$ to estimate A for that particular window. We then slide the window by Δt so that the starting data points in the next window are x_{i+1} and y_{i+1} and estimate A for this new window. This is repeated for the length of the time series. (iv) For each window, we calculate the eigenvalues of the corresponding estimated A, and using Eqs. (21) and (22) we calculate the eigenvalues of the Jacobian and the associated standard errors. (v) We plot the resulting estimated eigenvalues of the Jacobian as a function of the greatest value of $t = t_0 + (i+m)\Delta t$ for each sliding window in Figures 7 and 9.

A. Homoclinic bifurcation: No critical slow down, decreasing frequency

Our first example has dynamics described by

$$\ddot{x} + x^2 - \alpha = 0, \tag{25}$$

which is an autonomous second order ODE in one variable, x with control parameter α. We can rewrite this as two coupled first order ODEs as

$$\begin{aligned} \dot{x} &= y, \\ \dot{y} &= \alpha - x^2. \end{aligned} \tag{26}$$

The steady state solutions $(\dot{x}=0, \dot{y}=0)$ are $(x,y) = (\pm\sqrt{\alpha}, 0)$, therefore there are only steady state solutions for $\alpha \geq 0$. One can find the stability of these solutions by

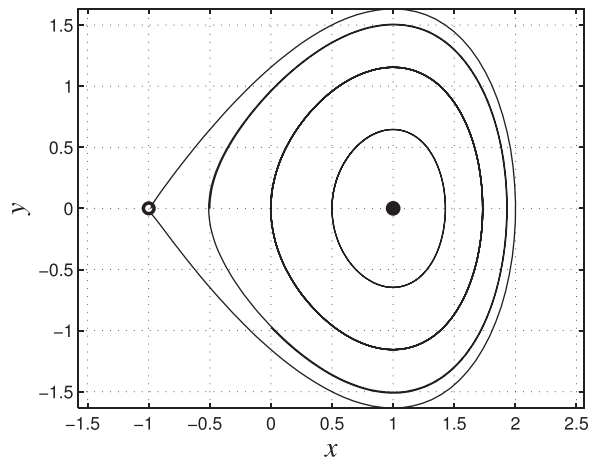

FIG. 4. Phase portrait for Eq. (26) with $\alpha = 1$. There is a saddle at $(x, y) = (-1, 0)$ and a center at $(x, y) = (1, 0)$. Surrounding the center is a continuum of stable orbits up until the outer homoclinic orbit that passes through the saddle point. Any initial condition lying outside the region enclosed by the homoclinic orbit is unstable.

looking at the eigenvalues of the Jacobian at these points. The Jacobian for this system is

$$J(x, y) = \begin{pmatrix} 0 & 1 \\ -2x & 0 \end{pmatrix}, \tag{27}$$

with eigenvalues

$$\lambda = \pm\sqrt{-2x}. \tag{28}$$

At $(-\sqrt{\alpha}, 0)$, $\lambda = \pm(4\alpha)^{1/4}$, so both eigenvalues are real, one being positive, the other negative so this is a saddle, and at the other fixed point $(\sqrt{\alpha}, 0)$, both eigenvalues are purely imaginary, , $\lambda = \pm i(4\alpha)^{1/4}$ indicating a center. This is a stable center since Eq. (25) is time reversal invariant, i.e., under the transformation $t \to -t$, the equation remains the same. One sees this must be stable if one considers an orbit starting from some point and watches the evolution of the point in two instances, one with time running backwards and one forwards. After some time, two evolving points must meet and repeat the same path exactly. One can conclude therefore that they must be closed, stable orbits and the system is conservative.

So there are a continuum of stable orbits surrounding the centre each with a different amplitude and frequency. These orbits remain stable unless they pass the other side of the saddle point. The orbit that intersects the saddle is known as a homoclinic orbit and has an infinitely long period. One can now draw the phase portrait of the system in Figure 4 and the evolution of the steady solutions with slowly varying α in Figure 5. By this we mean $\dot{\alpha} \ll (4\alpha)^{1/4}$, that is, the parameter varies much slower than the timescale of the system so that the system stays approximately in steady state. As α approaches zero from positive, real values, the continuum of orbits collides with the saddle point in a homoclinic bifurcation (a.k.a. saddle connection) at $\alpha = 0$.

We next introduce a Gaussian white noise term to each equation. That is Eq. (26) goes to $\dot{x} = y + \xi^{(x)}(t)$ and $\dot{y} = \alpha - x^2 + \xi^{(y)}(t)$. These noise terms also act as a small perturbation that helps reveal the system's Jacobian when the system is sitting at or near a fixed point. The effect of adding the noise term is to kick the system into the higher or lower orbits on each time step. When numerically integrating these equations in some instances, one finds the noise terms kick the system out of the stable region enclosed by the homoclinic orbit. This becomes more likely for larger amplitude noise and the closer one is to the bifurcation (smaller values of α as the homoclinic orbit shrinks). The particular integration of Eq. (25) shown in Figure 6 for the values of the parameters reported appears reasonably typical however.

From analytical analysis of the equations, we expect to see no critical slowing down as we approach the bifurcation by varying α, since there is no real part in the Jacobian's eigenvalues, however we should see a decrease in frequency proportional to $(4\alpha)^{1/4}$. For this system, this is our bifurcation indicator. We apply our method to the time series generated by Eq. (26) with slowly varying α ($\dot{\alpha} = -\frac{1}{500}$ and α varies linearly from $\frac{1}{5}$ and approaches 0) and noise standard

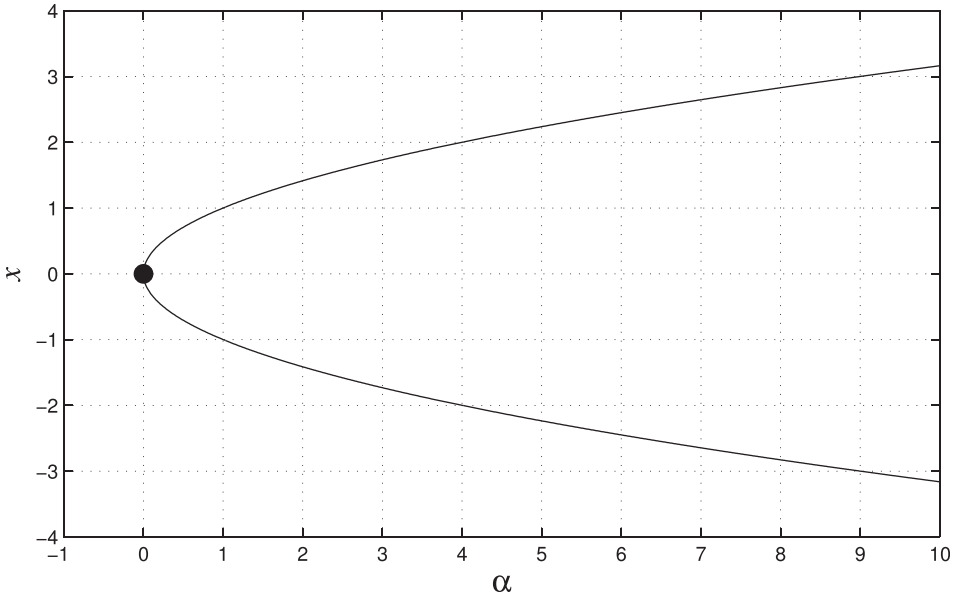

FIG. 5. Evolution of steady state solutions with slowly varying α for Eq. (26) projected onto the x axis ($y = 0$). The lower branch described by $x = -\sqrt{\alpha}$ is a saddle while the upper branch $x = \sqrt{\alpha}$ is a stable centre. These collide at $\alpha = 0$ in a homoclinic bifurcation (marked by the circle). There are no steady solutions for $\alpha < 0$.

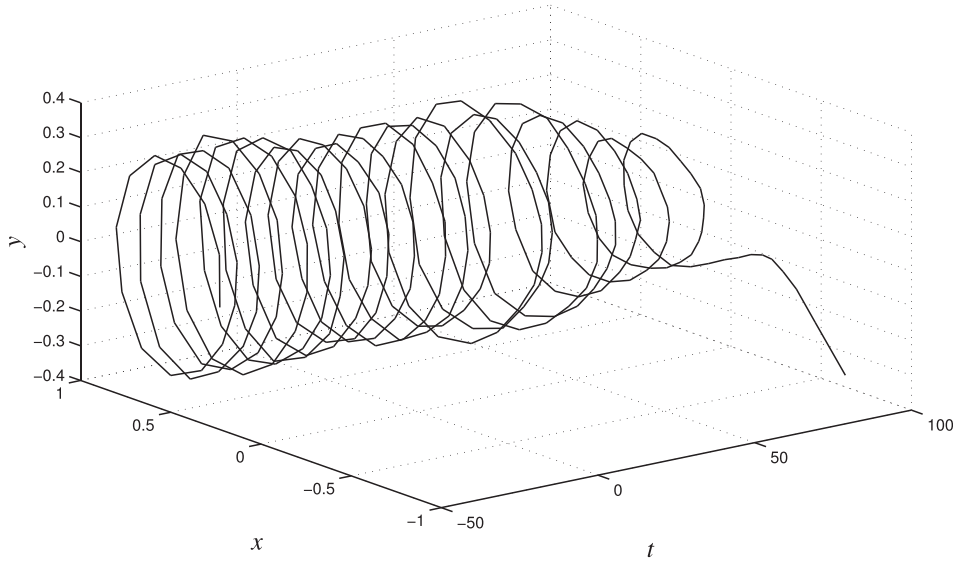

FIG. 6. Time series before bifurcation of variables x and y generated from Eq. (26) with slowly varying $\dot{\alpha} = -\frac{1}{500}$ and noise standard deviation $\sigma = 0.01$. To obtain the two time series of x and y, one projects this 3 dimensional plot on to each axis. In this region of (x, y), there is a centre surrounded by a continuum of stable limit cycles whose area gets smaller and closer to the saddle as time increases until the centre and the saddle collide in a homoclinic bifurcation at $t = 100$ ($\alpha = 0$).

deviation $\sigma = 0.01$ for both $\varepsilon^{(x)}$ and $\varepsilon^{(y)}$. Points in the time series are generated every $\Delta t = 0.5$. These time series are shown in Figure 6, and we fit a 2 variable AR(1) model to a sliding window of length $T_{window} = 50$ and compute the eigenvalues of A and hence determine J for each window. The real and imaginary parts of the reconstructed Jacobian's eigenvalues as a function of α are shown in Figure 7. There are two eigenvalues, each with real and imaginary parts, hence there are potentially four numbers that characterise these eigenvalues. However, they appear as a pair of complex conjugates since A is real and two dimensional so only two numbers, the real and imaginary parts of a single eigenvalue, describe A and therefore J. We see in this figure that the linear model we are fitting to this nonlinear time series reconstructs the Jacobian fairly well, i.e., the real part of the eigenvalues is approximately zero and the imaginary part equal to the frequency of oscillations decreases with decreasing α as we approach the homoclinic bifurcation.

The reader may be interested to note the typical physical systems these equations model. These equations are typical in mechanical systems and the bifurcation corresponds to "buckling."[27] That is a buckling system's dynamics are governed by $\ddot{x} + \delta\dot{x} + x^2 - \alpha = 0$. Our example is an idealisation where $\delta\dot{x}$, the damping term, is small or negligible. Neglecting the damping term does not significantly change the results apart from the addition of a small, constant damping term invariant to the bifurcation (no critical slowing down), turning the center into a weakly attracting spiral.

B. Hopf bifurcation: Critical slow down, no significant frequency change

Our second example shows a supercritical Hopf bifurcation at $\alpha = 0$, a transition from a stable spiral to a stable limit cycle, which is a local bifurcation and therefore shows critical slowing down. The equations in polar coordinates are

$$\begin{aligned} \dot{r} &= \alpha r - r^3, \\ \dot{\theta} &= 1 + r^2. \end{aligned} \tag{29}$$

There is a stable spiral at $r = 0$ when $\alpha < 0$ which becomes unstable at $\alpha > 0$. A stable limit cycle is born when $\alpha \geq 0$ at

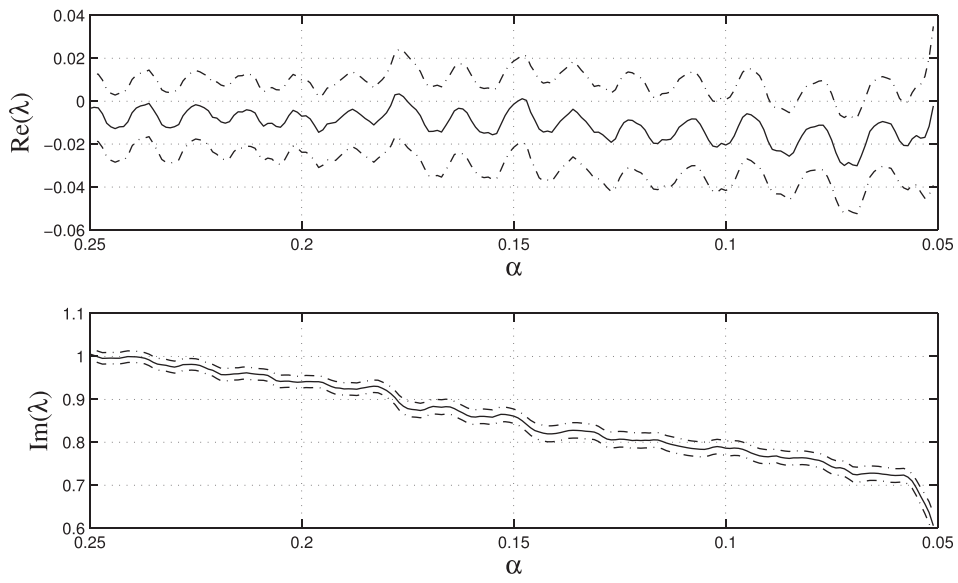

FIG. 7. Reconstruction of the real and imaginary parts of the Jacobian's eigenvalues from the time series in Figure 6 as a function of α. We use a sliding window of length $T_{window} = 50$ so that each window consists of $m = 100$ points. Dashed lines indicate upper and lower ranges of the standard error. There is no critical slowing down in this system as seen in the top panel, the decay rate given by the real part of the Jacobian's eigenvalues since this is a global bifurcation. However, the indicator of the approaching homoclinic bifurcation here is the slowing in frequency given by the imaginary part of the Jacobian's eigenvalues.

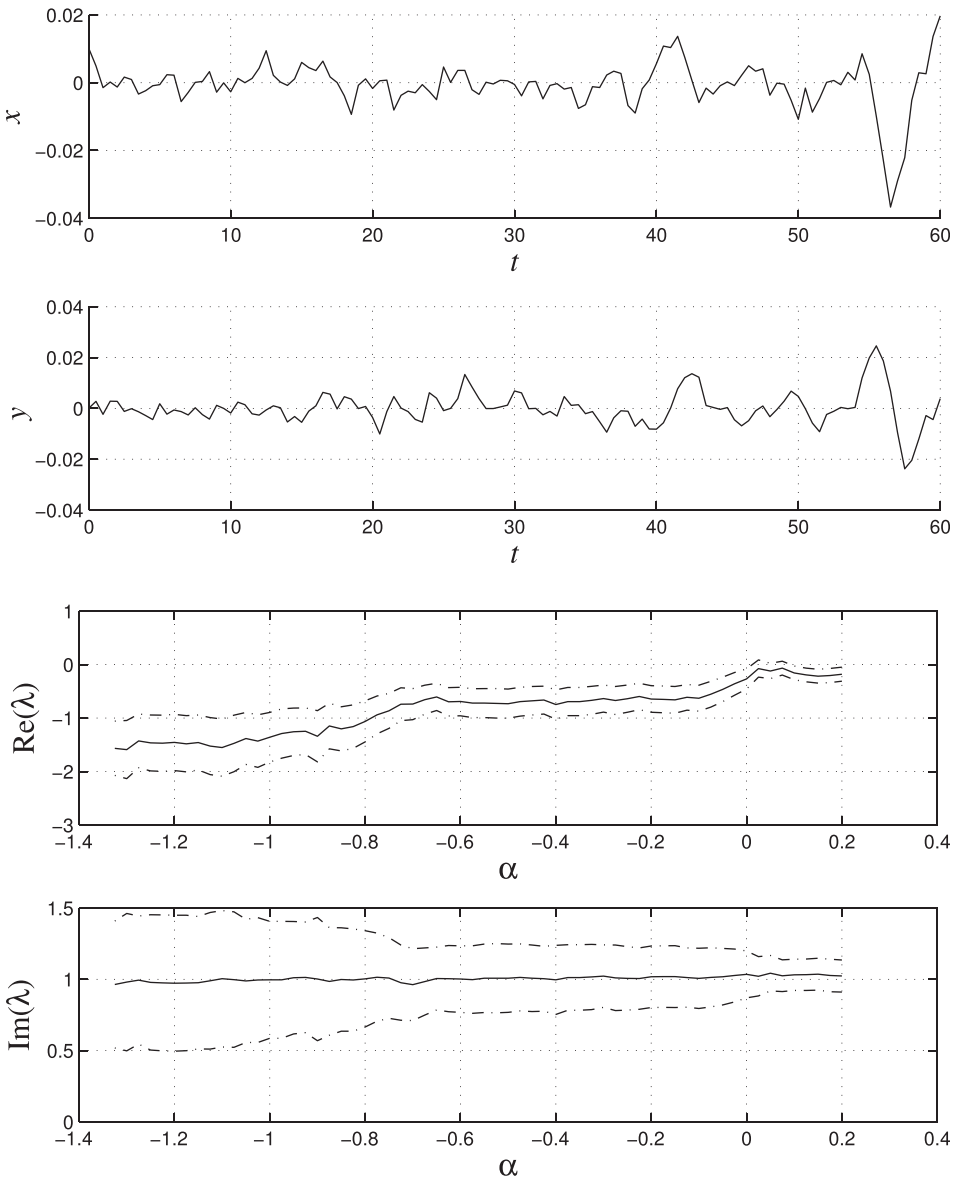

FIG. 8. Time series of variables x and y approaching the Hopf bifurcation generated from Eq. (29) with slowly varying $\dot{\alpha} = \frac{1}{20}$ and noise standard deviation $\sigma = 0.01$. A stable spiral becomes unstable resulting in a stable limit cycle following a Hopf bifurcation at $t = 58$ ($\alpha = 0$).

FIG. 9. Reconstruction of the real and imaginary parts of the Jacobian's eigenvalues from the time series in Figure 8 as a function of α. We use a sliding window of length $T_{window} = 30$ so that each window consists of $m = 60$ points. Dashed lines indicate upper and lower ranges of the standard error. One sees critical slowing down as expected from the increasing real part of the Jacobian's eigenvalues. There is no large frequency change visible here as we approach the bifurcation.

$r = \sqrt{\alpha}$. Rewriting the equations in cartesian coordinates using the transformations $x = r\cos\theta$ and $y = r\sin\theta$, we find the Jacobian at $(x, y) = (0, 0)$ is

$$J(0,0) = \begin{pmatrix} \alpha & -1 \\ 1 & \alpha \end{pmatrix}, \tag{30}$$

which has a pair of complex conjugate eigenvalues $\lambda = \alpha \pm i$. Therefore, as we vary α from negative values towards 0 we expect to see the real part of the Jacobian increasing from negative values until it reaches zero at $\alpha = 0$. The imaginary part of the Jacobian's eigenvalue should be 1. A pair of complex conjugate eigenvalues crossing from negative to the positive real half of the complex plane is the definition of a Hopf bifurcation.

Once again, we introduce a Gaussian white noise term to Eq. (29) as in the last example and compute the time series while slowly varying α ($\dot{\alpha} = \frac{1}{20}$, α varies linearly from -2.8 to 0.2) and equal noise standard deviation $\sigma = 0.01$ on both equations. Points in the time series are generated every $\Delta t = 0.5$. These time series are shown in Figure 8 and we fit a 2 variable AR(1) model to a sliding window of length $T_{window} = 30$ and compute the eigenvalues of A and hence determine J for each window. The real and imaginary parts of the reconstructed Jacobian's eigenvalues as a function of α are shown in Figure 9. From analytical analysis of the equations, we expect critical slowing down as we approach the bifurcation by varying α since the imaginary part in the Jacobian's eigenvalues is constant ($\mathbb{I}(\lambda) \sim 1$) while the real part is proportional to α. For the Hopf bifurcation, the real part of the Jacobian is our bifurcation indicator.

V. CONCLUSIONS

In this paper, we have generalized a method of detecting bifurcations in a noisy time series where the deterministic part of the fitted model is described by an autonomous first order ODE with one dynamical variable to models that are described by N coupled first order ODEs with N dynamical variables. These models are also general enough to include Nth order ODEs of one variable and nonautonomous systems by making a simple change of variables (or even

mixtures of the two). Our generalisation also allows bifurcation detection to be applied spatially if one treats each spatial location as a new dynamical variable. These techniques assume (i) the system from which the time series is generated is approximately in a steady state, (ii) any control parameter is slowly varying compared to the timescale of the system, and (iii) noise is white and uncorrelated with itself at other times and its amplitude is small. The technique fits a linear model with additive Gaussian white noise (AR(1) model) to the data. The dynamics are generally described sufficiently by such a minimal model provided perturbations from the steady state are small. The technique essentially reconstructs the eigenvalues of the system's effective Jacobian at its present coordinates with minimal knowledge about the system. Information about the eigenvalues of the system's Jacobian is potentially useful as the behaviour of these eigenvalues around many different bifurcations has been well studied.

In the $N=1$ case, one real eigenvalue can move along the real line corresponding simply to decay/growth type behaviour in the system (decay corresponds to negative values, growth to positive values). The movement of this eigenvalue from negative values towards zero indicates critical slowing down and reducing stability. The system may therefore be approaching a bifurcation and hence an abrupt change in its behaviour. This is the only type of behaviour modelled by $N=1$ however real dynamical systems may have much more complex behaviour. They can show oscillatory and chaotic dynamics as well as fixed point solutions. There are bifurcations between these three types of behaviour and some of them are global rather than local bifurcations and cannot be detected by the movement of the real part of the eigenvalue as we showed for the homoclinic bifurcation. Other examples of global bifurcations for $N=2$ that show no critical slowing down are the infinite period and saddle node bifurcation of cycles.[18,27] In the $N\geq 2$ case, one gets additional indicators from the N eigenvalues and, provided the system cannot be decoupled, some of these eigenvalues will be complex. The real and imaginary parts of these N eigenvalues all provide additional information on the behaviour of the system, the real parts telling one about the damping/growth rates along the associated eigenmodes and the imaginary parts telling one about the frequency of oscillation of that eigenmode. We showed that even though the homoclinic bifurcation cannot be detected by critical slowing down, it can be detected by the changing oscillation frequency.

Taken together this information about how these eigenvalues are evolving and their values can narrow down the possible type of approaching bifurcation and therefore something about the likely behaviour of the system following the bifurcation. To provide some examples for $N=2$ systems, there are some generic scaling laws when one is near the bifurcation. Some of these are listed in Table 7.4.1 of Strogatz's text,[18] and this may assist with identification of the type of bifurcation. Also Thompson and Sieber[29] provide a table of precursors to different types of bifurcation and classify them as being safe, explosive, or dangerous.

We anticipate that our extended method will prove useful in applications to the climate system, which has high dimensionality and is known to exhibit deterministic chaos on short, weather timescales as well as abrupt changes on longer, climate timescales. As an example of a potential application, consider the well studied Lorenz model, a simple model that shows transitions from fixed point to oscillatory to chaotic behaviour originally conceived as a simplified model of atmospheric convection.[30] It is described by a $N=3$ model, the dynamical equations for each given by $\dot{x}=\sigma(y-x)$, $\dot{y}=rx-y-xz$ and $\dot{z}=xy-bz$. The parameters σ and b are usually fixed to $\sigma=10$ and $b=\frac{8}{3}$, and r is the varied control parameter. Imagine we do not know the underlying dynamical model and we only have access to the noisy time series generated by the Lorenz equations. We apply our technique and reconstruct the Jacobian of this model. What would we be able to say about the dynamics? We consider the bifurcation from oscillatory to chaotic regimes, a subcritical Hopf bifurcation occurring at $r_H\sim 24.7$ around the fixed points $(x,y,z)=(\pm\sqrt{b(r-1)},\pm\sqrt{b(r-1)},r-1)$ (see Ref. 18 for example, for more information about the Lorenz model). Around this bifurcation, there are a pair of complex conjugate eigenvalues located in the negative real half of the complex plane and a third purely real eigenvalue sitting on the negative real line much further away from the origin. We assume we are close to one of the fixed points $(\pm\sqrt{b(r-1)},\pm\sqrt{b(r-1)},r-1)$ as we vary $r>0$ slowly towards r_H. Therefore, from the reconstructed Jacobian, we expect an attracting spiral on the plane spanned by the two eigenvectors associated to the complex conjugate pair of eigenvalues for $r<r_H$. In the third orthogonal direction given by the third eigenvector, we expect any displacement in this direction to be damped back towards the attracting spiral plane as the eigenvalue associated to it is purely real and much more negative. After the Hopf bifurcation, $r>r_H$, the two complex eigenvalues cross to the positive real side of the complex plane resulting in the spiral becoming unstable and the onset of chaos. We could then conclude from the reconstructed Jacobian that the spiral would become unstable but we would not know the dynamics would become chaotic. We could also conclude the unstable dynamics is mostly still confined to the same two dimensional spiral plane since the third eigenvalue remains real and negative. This illustrates that by looking at the evolution of the eigenvalues one can anticipate something about future behaviour of the system, although not everything.

Even though one could use a very large N model, in practice a small N model will probably capture most of the important features of the system. In practice if one did fit a large N model, one would probably find there were a few large eigenvalues of A. These eigenvalues dominate the dynamics, and therefore one could project on to the eigenvectors corresponding to these large eigenvalues and still have a good representation of the system while reducing the complexity. Using a large N model also negates most of the appeal of using these relatively simple statistical techniques.

ACKNOWLEDGMENTS

The research leading to these results has received funding from the European Union Seventh Framework Programme FP7/2007-2013 under Grant Agreement No. 603864 (HELIX). We thank Jan Sieber for help in identifying the case studies and useful comments on an early draft of the manuscript.

[1]M. Scheffer, J. Bacompte, W. A. Brock, V. Brovkin, S. R. Carpenter, V. Dakos, H. Held, E. H. van Nes, M. Rietkerk, and G. Sugihara, Nature **461**, 53 (2009).
[2]T. M. Lenton, Nat. Clim. Change **1**, 201 (2011).
[3]M. Scheffer, S. R. Carpenter, T. M. Lenton, J. Bascompte, W. Brock, V. Dakos, J. van de Koppel, I. A. van de Leemput, S. A. Levin, E. H. van Nes *et al.*, Science **338**, 344 (2012).
[4]C. Wissel, Oecologia **65**, 101 (1984).
[5]S. Carpenter, J. Cole, M. L. Pace, R. Batt, W. A. Brock, T. Cline, J. Coloso, J. R. Hodgson, J. F. Kitchell, D. A. Seekell *et al.*, Science **332**, 1079 (2011).
[6]A. J. Veraart, E. J. Faassen, V. Dakos, E. H. van Nes, M. Lurling, and M. Scheffer, Nature **481**, 357 (2012).
[7]S. Rahmstorf, M. Crucifix, A. Ganopolski, H. Goosse, I. Kamenkovich, R. Knutti, G. Lohmann, R. Marsh, L. A. Mysak, Z. Wang *et al.*, Geophys. Res. Lett. **32**, L23605, doi:10.1029/2005GL023655 (2005).
[8]E. Hawkins, R. S. Smith, L. C. Allison, J. M. Gregory, T. J. Woollings, H. Pohlmann, and B. de Cuevas, Geophys. Res. Lett. **38**, L10605, doi:10.1029/2011GL047208 (2011).
[9]V. Dakos, M. Scheffer, E. H. van Nes, V. Brovkin, V. Petoukhov, and H. Held, Proc. Natl. Acad. Sci. U.S.A. **105**, 14308 (2008).
[10]H. Held and T. Kleinen, Geophys. Res. Lett. **31**, L23207, doi:10.1029/2004GL020972 (2004).
[11]V. N. Livina and T. M. Lenton, Geophys. Res. Lett. **34**, L03712, doi:10.1029/2006GL028672 (2007).
[12]T. M. Lenton, R. J. Myerscough, R. Marsh, V. N. Livina, A. R. Price, S. J. Cox, and G. Team, Philos. Trans. A **367**, 871 (2009).
[13]C. A. Boulton, L. C. Allison, and T. M. Lenton, Nat. Commun. **5**, 5752 (2014).
[14]T. M. Lenton, V. N. Livina, V. Dakos, E. H. van Nes, and M. Scheffer, Philos. Trans. R. Soc. A **370**, 1185 (2012).
[15]P. D. Ditlevsen and S. J. Johnsen, Geophys. Res. Lett. **37**, L19703, doi:10.1029/2010GL044486 (2010).
[16]A. A. Cimatoribus, S. S. Drijfhout, V. Livina, and G. van der Schrier, Clim. Past **9**, 323 (2013).
[17]C. A. Boulton, P. Good, and T. M. Lenton, Theor. Ecol. **6**, 373 (2013).
[18]S. H. Strogatz, *Nonlinear Dynamics and Chaos* (Westview Press, 2001).
[19]Y. A. Kuznetsov, *Elements of Applied Bifurcation Theory*, 3rd ed. (Springer, 2004).
[20]M. Crucifix, Philos. Trans. R. Soc. A **370**, 1140 (2012).
[21]P. Ashwin and P. Ditlevsen, "The Middle Pleistocene transition as a generic bifurcation on a slow manifold," Climate Dynamics (to be published).
[22]B. K. Øksendal, *Stochastic Differential Equations: An Introduction with Applications* (Springer, 2003).
[23]K. Bichteler, *Stochastic Integration with Jumps* (Cambridge University Press, 2010).
[24]P. E. Kloeden and E. Platen, *Numerical Solution of Stochastic Differential Equations* (Springer, 1992).
[25]H. von Storch and F. W. Zwiers, *Statistical Analysis in Climate Research* (Cambridge University Press, 1999).
[26]H. Lütkepohl, *Introduction to Multiple Time Series Analysis* (Springer-Verlag, 1991).
[27]J. M. T. Thompson and H. B. Stewart, *Nonlinear Dynamics and Chaos*, 2nd ed. (John Wiley and Sons, Ltd., 2002).
[28]J. H. Wilkinson, *Rounding Errors in Algebraic Processes* (Her Majesty's Stationary Office, 1963).
[29]J. M. T. Thompson and J. Sieber, Int. J. Bifurcation Chaos **21**, 399 (2011).
[30]E. N. Lorenz, J. Atmos. Sci. **20**, 130 (1963).